JRRD Volume 41, Number 6A, Pages 775–786
November/December 2004
Journal of Rehabilitation Research & Development

Finite-element analysis to determine effect of monolimb flexibility on structural strength and interaction between residual limb and prosthetic socket

Winson C. C. Lee, BSc; Ming Zhang, PhD; David A. Boone, CP, BS, MPH; Bill Contoyannis, MEngSc
Jockey Club Rehabilitation Engineering Centre, The Hong Kong Polytechnic University, Hong Kong, China; REHABTech, Monash University, Melbourne, Australia

Abstract—Monolimb refers to a kind of transtibial prostheses having the socket and shank molded into one piece of thermoplastic material. One of its characteristics is that the shank is made of a material that can deform during walking, which can simulate ankle joint motion to some extent. Changes in shank geometry can alter the stress distribution within the monolimb and at the residual limb-socket interface and, respectively, affect the deformability and structural integrity of the prosthesis and comfort perceived by amputees. This paper describes the development of a finite-element model for the study of the structural behavior of monolimbs with different shank designs and the interaction between the limb and socket during walking. The von Mises stress distributions in monolimbs with different shank designs at different walking phases are reported. With the use of distortion energy theory, possible failure was predicted. The effect of the stiffness of the monolimb shanks on the stress distribution at the limb-socket interface was studied. The results show a trend—the peak stress applied to the limb was lowered as the shank stiffness decreased. This information is useful for future monolimb optimization.

Key words: finite-element analysis, interface pressure, interface shear stress, monolimb, shank flexibility, structural integrity, transtibial prosthesis.

INTRODUCTION

Transtibial amputees usually demonstrate some gait abnormalities such as lower walking speed [1], increased energy cost [2], and asymmetries between legs of unilateral amputees in stance phase time, step length, and vertical peak force [3]. The gait abnormalities are believed to be due mainly to the loss of active dorsiflexion and plantar-flexion motions of the ankle joint [4]. Prostheses have been designed to compensate for the loss of motion at the foot by an incorporation of energy storing and releasing (ESAR) capabilities with the use of flexible keels or shanks. The Seattle foot™ and FlexFoot™ are examples of ESAR prosthetic components. Previous research suggested that many amputees subjectively prefer ESAR prosthetic feet to conventional solid ankle cushion heel (SACH) feet for normal and fast walking [5,6]. However, many amputees still use the simple SACH feet because of their lower cost.

Abbreviations: CAD/CAM = computer-aided design/computer-aided manufacturing, COP = center of pressure, ESAR = energy storing and releasing, FE = finite element, GRF = ground reaction force, MRI = magnetic resonance imaging, SACH = solid ankle cushion heel.

This material was based on work supported by The Hong Kong Polytechnic University Research Studentship and a grant from the Research Grant Council of Hong Kong (project PolyU 5200/02E).

Address all correspondence to Ming Zhang, PhD; Jockey Club Rehabilitation Engineering Centre, The Hong Kong Polytechnic University, Hong Kong, P.R. China; 852-2766-4939; fax: 852-2362-4365; email: rcmzhang@polyu.edu.hk.

DOI: 10.1682/JRRD.2004.01.0003

A "monolimb" prosthesis design using a conventional prosthetic foot such as a SACH foot, if properly designed, perhaps is an alternative to ESAR prosthetic feet, providing elastic response of the shank [7], while at the same time lowering the total prosthetic weight and cost. A monolimb is a kind of transtibial prosthesis having the socket and the shank molded into one piece of thermoplastic material. Different names have been used for this kind of prosthesis, including endoflex [7], total thermoplastic prosthesis [8], and ultralight prosthesis [9]. Because of the elasticity of thermoplastics, the shank can deform, leading to simulated dorsiflexion and plantarflexion of the prosthetic foot. By proper use of material and structural design, the shank deformability can be altered to mimic natural ankle joint motions. At the same time, structural integrity should be maintained without permanent deformation and buckling of the prosthesis. Changes in shank flexibility may alter the stress distribution at the prosthetic socket-residual limb interface, which is related to the comfort perceived by the amputees [10]. Until now, no clear guideline has been written on the shank designs of monolimbs. Essential for optimizing the design of the monolimb and maximizing comfort are a comprehensive understanding of the deformation and stress at the shank of the monolimb during walking and the effect of shank flexibility on stress distribution at the interface between socket and limb.

In general, two approaches exist to investigating shank deformation and its effect on socket-limb interface stress: experimental measurements and theoretical analyses. Experimental measurements require the use of stress/strain sensors attached to appropriate positions of the shank and the socket inner surface. Theoretical analyses such as finite-element (FE) methods, which have been widely used in lower-limb prosthetics in the past decade, can be useful to study the deformations and stresses. The advantage of the use of FE analysis is that stress, strain, and motion in any parts of the model can be predicted and parametric analyses can be performed easily without the need to fabricate prostheses. In previous FE models, the focus was on investigating the variation of stresses distributed at the limb-socket interface under different socket modifications [11–12], material properties of the sockets [11,13] and liners [14], and frictional properties at the interface [15]. The deformability of the prosthesis and the effect of shank deformation on interface stresses received little attention.

This paper describes the development of an FE model that was used to study the interface stress between the limb and socket, shank flexibility, and possible failure of the prosthesis. Different shank geometries were used and their effects on limb-socket interface stresses studied.

METHODS

We developed an FE model for a right-sided unilateral transtibial amputee subject to determine the stresses in the monolimb during walking and the effect of shank stiffness on interface stresses at the limb-socket interface. The subject, 55 years old and 81 kg, had experience using monolimbs. Contact between the limb and the socket was simulated, considering prestress when the limb was donned into a shape-modified socket and friction/slip with the use of an automated contact technique. Our previous FE analyses showed the importance of considering prestress in predicting interface stresses at loading stage [16–17]. Proximal regions of soft tissue and bones were fixed, and loading was applied at the prosthetic foot according to gait analysis data [17–19].

Geometries

The geometries of the bones and their positions relative to the limb surface were obtained by magnetic resonance imaging (MRI) of the subject. Outlines of bones were identified in Mimics 7.1 (Materialise, Leuven, Belgium). We obtained the residual limb surface by digitizing a loose plaster cast using the BioSculptor™ system. Bone geometries were assembled into the residual limb according to the MRI. A prosthetist using ShapeMaker™ 4.3 (Seattle System, Poulsbo, WA) prepared the geometry of the monolimb, applying a built-in, shape-rectification template, as shown in **Figure 1**, to the digitized limb surface and aligning a shank and blending smoothly to the socket end. Different geometries of shanks (**Figure 2**) were designed for analysis. The whole monolimb was assigned 4 mm thickness. The geometry of the prosthetic foot was based on direct measurement of a Kingsley SACH foot (length 250 mm) and was added to the distal end of the shank. The foot was partitioned into two regions: the wooden keel and the surrounding rubber foam. Although the shank geometry was varied in different designs, the relative positions of the prosthetic foot to the socket were the same. The model in its entirety, as shown in **Figure 3(a)**, was exported to ABAQUS 6.3 (Hibbitt, Karlsson & Sorensen, Inc., Warwick, RI). An FE mesh with three-dimensional tetrahedral elements

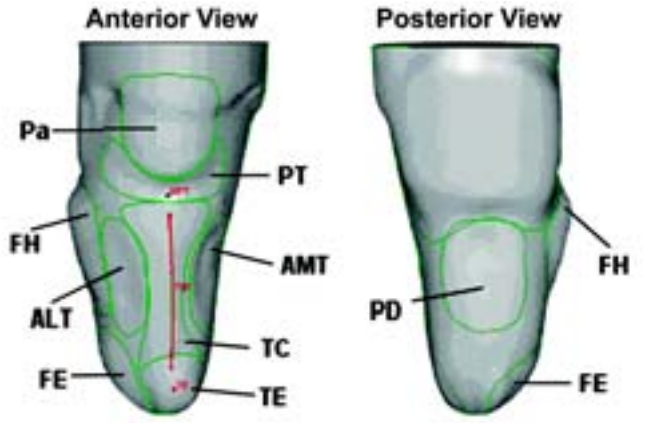

Pa	PT	FH	AMT	ALT	TC	FE	TE	PD
2	–7	7	–4	–3	3	4	7	–7

Figure 1.
Socket rectification template. Patella (Pa), patellar tendon (PT), fibular head (FH), anteromedial tibia (AMT), anterolateral tibia (ALT), tibial crest (TC), fibular end (FE), tibial end (TE), and popliteal depression (PD) are regions where rectifications were applied. Numbers show maximum depth/height (mm) of undercuts (negative values) or buildups (positive values) over regions.

was built with ABAQUS automeshing techniques. The number of elements assigned varied among the different monolimb designs, ranging from 37,836 to 38,565.

Material Properties

In this preliminary study, we assumed the mechanical properties of the materials to be linearly elastic, isotropic, and homogeneous. The estimated Young's modulus was 200 kPa [15] for soft tissues and 1500 MPa [20] for the monolimb structure, following the mechanical properties of polypropylene homopolymer. Poisson's ratio was assumed to be 0.45 for soft tissues and 0.3 for the monolimb. The prosthetic foot was partitioned into a keel region and surrounding rubber foam, and these were assigned Young's moduli of 700 MPa and 5 MPa, respectively. Poisson's ratio was assumed to be 0.3 for the two regions of the prosthetic foot.

Boundary Conditions and Analysis

The four bones were given fixed boundaries. A fixed boundary was also given to the proximal region of the soft tissue, as shown in **Figure 3**. The fixed region of the soft tissue was away from the socket so that the boundary

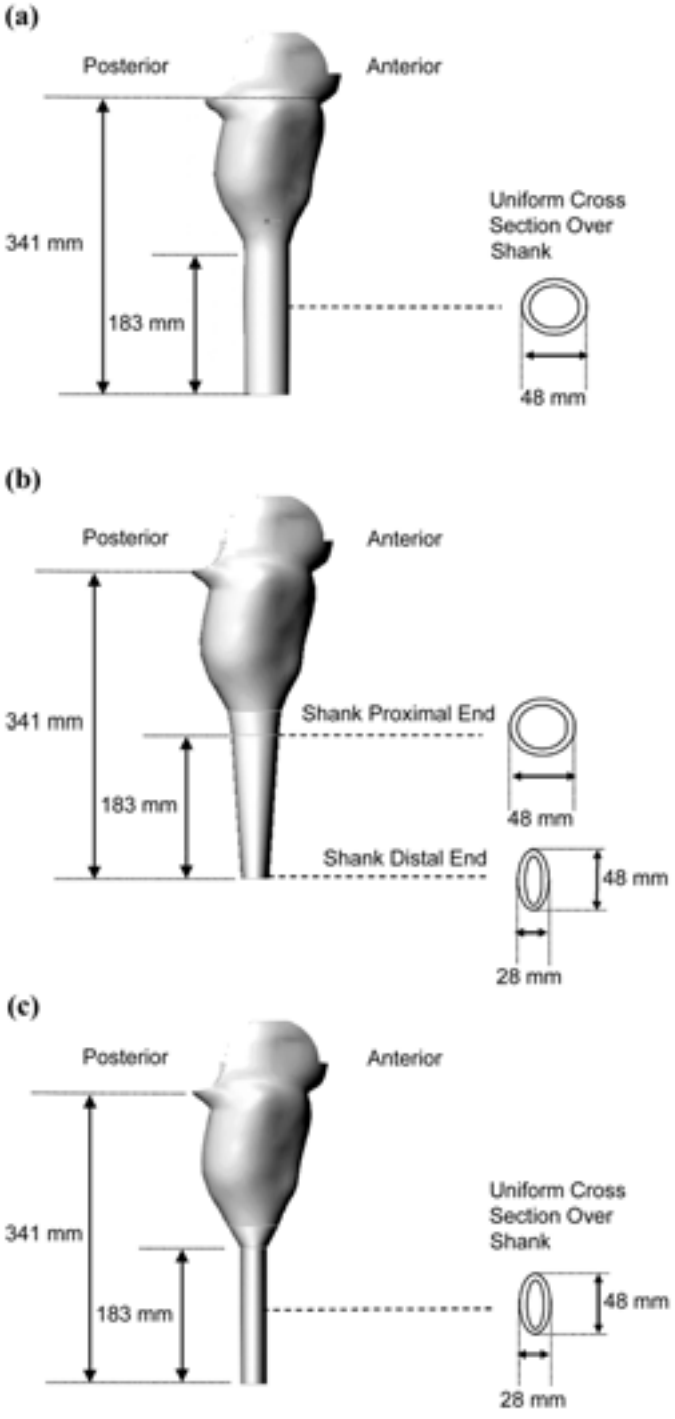

Figure 2.
Three different shank designs analyzed in finite-element model: **(a)** Design A, circular shank with outer diameter 48 mm; **(b)** Design B, proximal end of shank circular with outer diameter of 48 mm, cross section becoming elliptical toward distal end as anteroposterior dimension linearly reduces to 28 mm; and **(c)** Design C, elliptical shank with outer diameter of 28 mm.

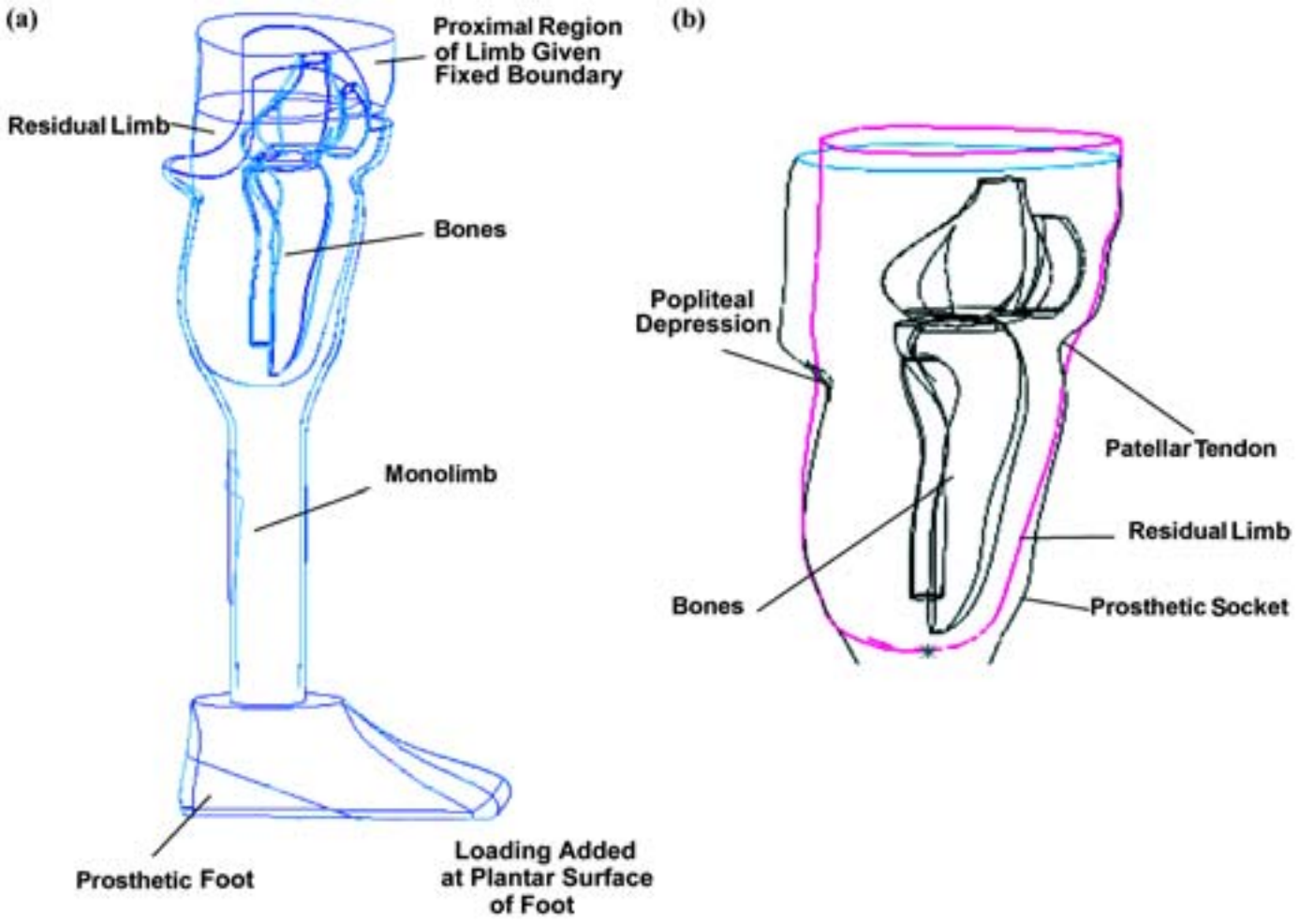

Figure 3.
(a) Geometries of bones, residual limb, monolimb, and prosthetic foot and **(b)** closer look at residual limb-prosthetic socket showing that some regions of undeformed residual limb penetrated into socket because of socket rectification.

condition would not significantly affect interface stresses. The bones and soft tissues were modeled as one body with different mechanical properties. The residual limb and socket were modeled as two separate structures, and their interaction was simulated with the use of automated contact methods. We tied together the distal surface of the shank and the top surface of the prosthetic foot by rigidly connecting the nodes between the two surfaces where they made contact. For simplification, we assumed that no foot clamp adaptor held the shank onto the prosthetic foot.

The analysis had two phases. The first phase was to simulate the interaction produced by donning the limb into the prosthetic socket. At this phase, the external surface of the monolimb, together with the bones and the soft tissue around the femur, were fixed. Initially, some regions of the limb penetrated into the prosthetic socket, as shown in **Figure 3(b)**, because of the socket rectification. An automated contact method was employed, and the solver in ABAQUS automatically moved the penetrated limb surface onto the inner surface of the socket. Stresses were developed on both the inner surface of the socket and the residual limb over the overlapped regions [16–17].

In the second phase, the prestresses and deformations calculated in the first phase were retained. The fixed boundary constraint previously added to the external surface of the monolimb was removed. External loadings were applied at the prosthetic foot to simulate the subject

walking. Stiffness changes upon large deformations, known as geometrical nonlinearity, were considered. Three load conditions were applied separately at the centers of pressure (COPs) on the plantar surface of the foot according to gait analysis data of the same amputee [18–19] to simulate heel strike, loading response, and heel-off gait—respectively, 8 percent, 19 percent, and 43 percent of stride. The COP was obtained by projecting the positions of COP calculated on the force platform onto the plantar surface of the foot. Kinematic data of the limb and monolimb and ground reaction forces (GRFs) were obtained with the Vicon Motion Analysis System and a force platform, respectively. The magnitude, position, and direction of the applied load are listed in **Table 1**. The loadings were assumed to be the same for different shank designs at the same loading conditions. This assumption was based on previous research showing that the GRFs varied little with the use of different stiffnesses of prosthetic feet [21–22]. Coefficient of friction (μ) of 0.5 was assigned for socket-limb interface [15,23]. Sliding was allowed only when the shear stress at the interface exceeded the critical shear stress value $\tau > \tau_{crit} = p$, where p is the value of normal stress. The analysis was performed with different shank designs of the monolimb, as shown in **Figure 2**.

RESULTS AND DISCUSSION

Figure 4 shows the von Mises stress distribution in the monolimb with a circular shank (Design A, **Figure 2**) over the three loading conditions. At heel strike and loading response, peak von Mises stresses fall on the anterior-proximal region of the shank. At heel off, peak von Mises stresses fall on the anterior-distal region of the shank. The stresses are smaller at heel strike because of the lower GRFs and shorter moment arm from the load line of the GRF to the shank and reach the highest—11.2 MPa for Design A—at heel off. Using distortion energy theory, which is widely used in predicting failure of ductile materials [24], we predicted failure to occur if the von Mises stress is equal to or greater than the uniaxial failure stress. The yield stress of polypropylene homopolymer, 35 MPa [20], is considered to be the uniaxial failure stress because the design of monolimb is deemed unacceptable if the permanent deformation occurs, changing the alignment of the prosthetic foot relative to the socket. Because the peak von Mises stresses are much lower than the yield stress of the thermoplastic material, we predicted that failure would not occur during level walking for that design. **Table 2** shows the values of prosthetic foot dorsiflexion angles. Foot dorsiflexion angles are defined here as the angle changes between the transverse plane and the flat surface of the prosthetic foot attached to the shank (**Figure 5**) after external loadings were added. The foot dorsiflexion angles take into account the motions of the prosthetic foot due to deformation of the shank and the movement of the whole monolimb with respect to the residual limb. For monolimb Design A, the prosthetic foot dorxiflexes to 4.2° at heel off, which is much lower than the normal foot dorsiflexion angle of around 10° [25] during heel off.

These results show a need for an increase in shank flexibility: the peak von Mises stresses were much lower than the yield stress of the material, the shank appears rigid for the circular shank with 48 mm outer diameter, and previous research showed that shank flexibilities can enhance gait performance [7,9]. We altered shank flexibilities in this study by changing the cross-sectional geometry of the shank, as shown in **Figure 2**. **Table 2** shows the locations of peak stress at the shank and compares the magnitudes of peak von Mises stresses and foot dorsiflexion angles among different shank designs at the three loading conditions. Reducing the anteroposterior dimension of the shank at the distal end (Design B) leads to increases in flexibility of the shank. High von Mises stresses (**Table 2**) and major deformation (**Figure 5(a)**) occur at the distal end of the shank of monolimb Design

Table 1.
Three loading conditions analyzed in finite-element model.1111

Loading Conditions (% of Stride)	Vertical Force (N)	Anteroposterior Force (N)*	Medial-Lateral Force (N)†	Center of Pressure Distance from Back of Heel (cm)
Heel Strike (8%)	480	–67	–10	5.3
Loading Response (19%)	946	–143	69	12.0
Heel Off (43%)	804	57	65	17.3

*Positive value indicates anterior-directed force.
†Positive value indicates lateral-directed force.

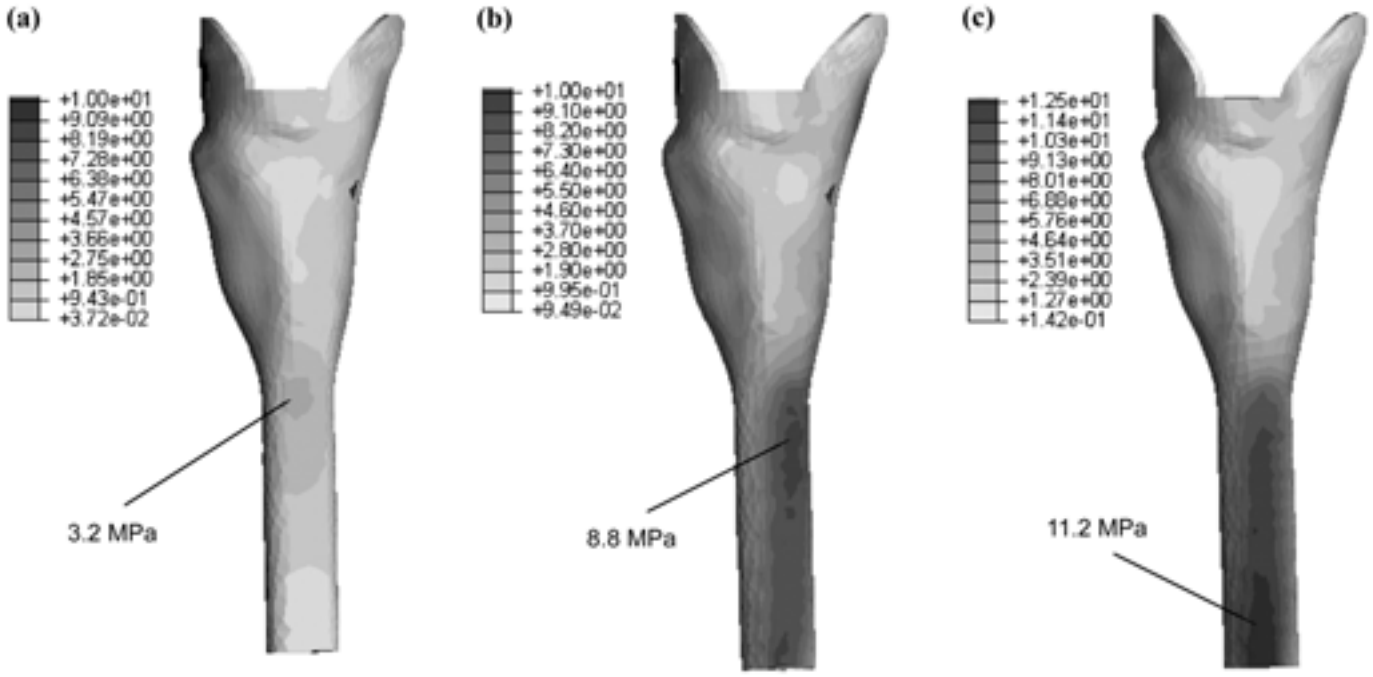

Figure 4.
von Mises stress distribution at monolimb with 48 mm-diameter circular shank (Design A) at **(a)** heel strike, **(b)** loading response, and **(c)** heel off.

Table 2.
Comparisons of peak von Mises stresses and foot dorsiflexion angles among three different shank designs at three loading conditions.2222

Conditions	Design	Location of Shank with Peak von Mises Stress	Peak von Mises Stress (MPa)	Foot Dorsiflexion Angle (°)
Heel Strike	A	Anterior-proximal	3.2	0.5
	B	Anterior-proximal	4.4	2.0
	C	Anterior-proximal	6.9	2.2
Loading Response	A	Anterior-proximal	8.8	2.7
	B	Anterior-distal	18.0	5.2
	C	Anterior-proximal	27.2	12.2
Heel Off	A	Anterior-distal	11.2	4.2
	B	Anterior-distal	30.8	11.5
	C	Anterior-distal	36.7	16.3

B at loading response and heel off. The peak von Mises stress for Design B increases to 30.8 MPa (**Table 2**) at heel off; this peak stress is predicted to be lower than the yield stress of the material, hence the design meets the strength requirement. Further investigation into the fatigue life of the monolimb under this stress level is required. Foot dorsiflexion angle reaches 11.5°, comparable to that of a normal foot at heel off. The increase in foot dorsiflexion angle at heel off could be the main contribution to the improved gait efficiency in a prosthesis with a flexible shank, as suggested by previous researchers [7,9,26]. Reducing the anteroposterior dimension of the shank at the proximal end, forming a uniform cross-sectional elliptical shank (Design C), further increases flexibility. However, some material yield is predicted to occur at heel off for the elliptical design, because the

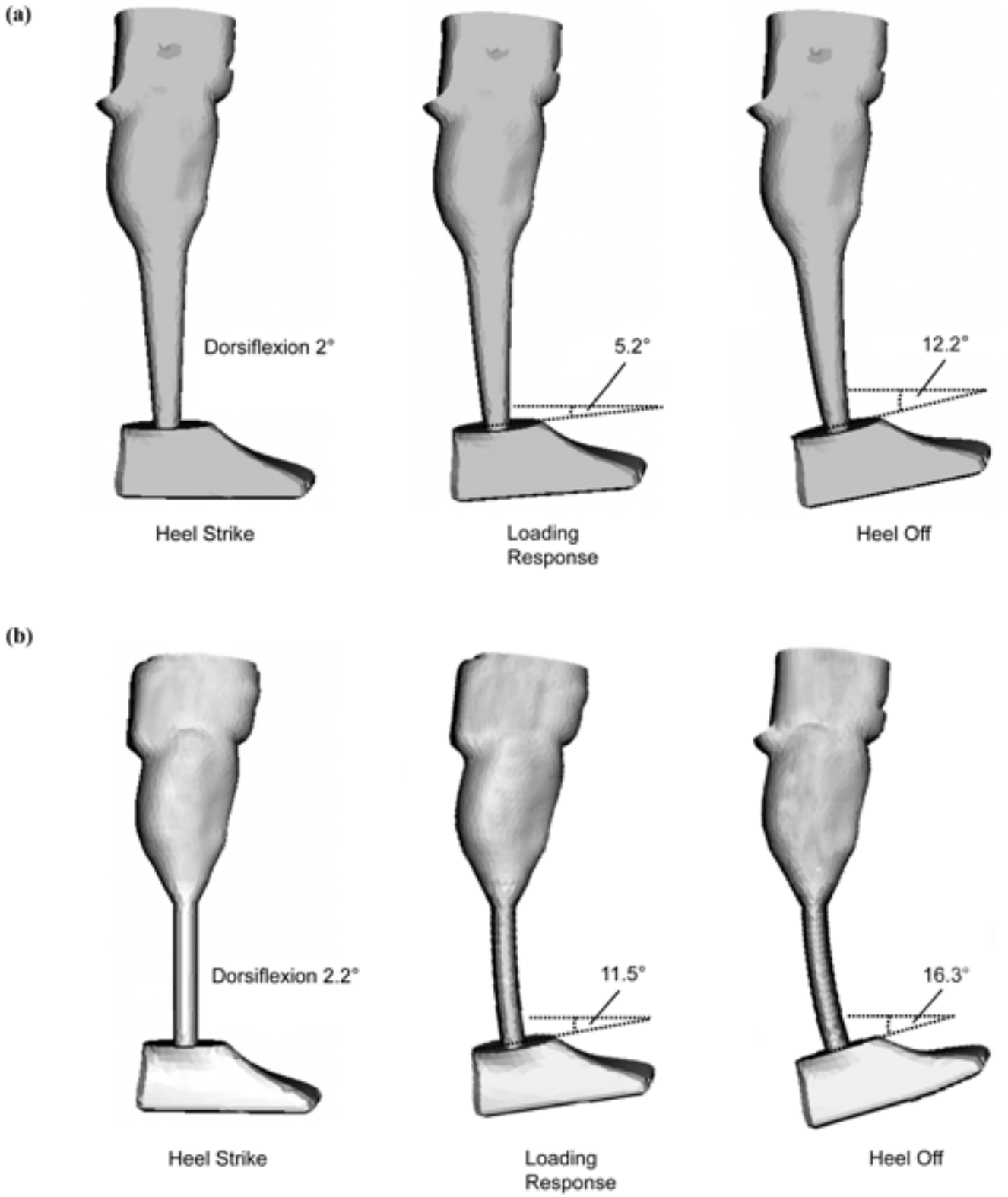

Figure 5.
Deformation of shank of **(a)** Design B and **(b)** Design C at three loading conditions.

peak von Mises stress was estimated to be slightly greater than 35 MPa. **Figure 5(b)** shows the predicted deformation of monolimb Design C.

It is notable that the measurement method of ankle motion used in this study is not same as the one used in gait analysis. Ankle motion is described in this study by the angle changes of the top surface of the solid wooden keel of the prosthetic foot in the sagittal plane. This measurement method emphasizes the motion of the prosthetic foot due to shank deflection, which was the primary interest of this study. The measured foot motion was apparently unaffected by the deformation of the rubber foam at the plantar region of the prosthetic foot and the possible motion between the shoe and the foot. In gait analysis, ankle motions are commonly measured according to the reflective markers attached to the prosthesis and the shoe. Motion of the foot-shoe complex and the compression of the rubber foam could both contribute to the foot motion.

Previous gait analyses show a brief external plantarflexion moment early in the stance phase as the line of action of the GRF passes posterior to the ankle joint, followed by a dorsiflexion moment when the GRF shifts anteriorly [25]. Our results, however, show that the prosthetic foot dorsiflexed at all the three loading conditions. At heel strike, the line of action of the ground reaction force as usual passes posterior to the ankle joint, which tends to plantarflex the prosthetic foot. However, as the force line passes anterior to the proximal shank and the knee joint, the foot dorsiflexion angle, defined as the angle changes between the transverse plane and the flat surface of the prosthetic foot attaching to the shank, is positive given the deformability of the shank as well as the motion of the monolimb relative to the residual limb. The magnitudes of the dorsiflexion angles are small at heel strike for the three monolimb designs.

Another important aspect of this study is to investigate the stress distribution at the limb-socket interface with varying monolimb flexibility. **Figure 6** shows the normal stress distributions of the limb at heel strike, loading response, and heel off with monolimb Design A. High pressure falls on the mid-patellar tendon, anterolateral tibia, anteromedial tibia, and popliteal depression regions where socket undercuts were made. The three loading conditions caused extension of the monolimb relative to the residual limb. The extension moment is consistent with previous gait study showing that transtibial amputees demonstrated an external knee extension moment almost throughout the stance phase of the gait because they tended to move the body center of mass more anteriorly [27]. Because of the extension moment of monolimb and the inward budge of the patellar bar, the stresses are greater in the patellar tendon region than in the popliteal depression region. The presence of laterally directed GRF [26] explains the higher pressure in anterolateral tibia than anteromedial tibia regions. High resultant shear stress, which is the combination of longitudinal and circumferential components of shear stresses in the plane of contact interface, is predicted at the four critical regions with socket undercuts. The peak stresses predicted in the FE model are in the range of the clinical measurements [28–29].

The patterns of the normal and shear stress distribution are similar among the three different shank designs at the same loading conditions, but differ in peak stress values. **Figures 7** and **8** compare the peak normal and resultant stress distributions over the four critical areas among different shank designs. Increases in shank flexibility tend to lead to general decreases in peak stresses applied onto the residual limb. The tendency could be explained from a total energy point of view. Deformation of the prosthesis absorbs some energy, just like the ESER prosthetic foot absorbs some potential energy, causing the reduction of the energy actually transferred to the residual limb. The magnitude of stresses applied onto the skin surface of the residual limb are related to the comfort perceived by amputees [10]. The reduction of stresses could explain the improved comfort of using prosthesis with flexible components [7,9,11].

We assumed in the model that the soft tissue was a passive structure. However, in reality, the muscles at the residual limb would have some degree of contractions during walking. Muscle contractions leading to stiffness changes at different regions of the limb could alter the stress distribution at the limb-socket interface. Little is known about the effect of muscle contractions on interface stresses because most FE models did not consider muscle contraction [11digitized15]. The inclusion of muscle contraction in the FE model requires the investigation of the timing and intensity of muscle contraction at the residual limb during walking, the relationship between muscle contraction and stiffness, and the muscle geometry from imaging data. The difference in prediction of interface stress between a passive soft tissue structure and a soft tissue with muscle contraction deserves further investigation.

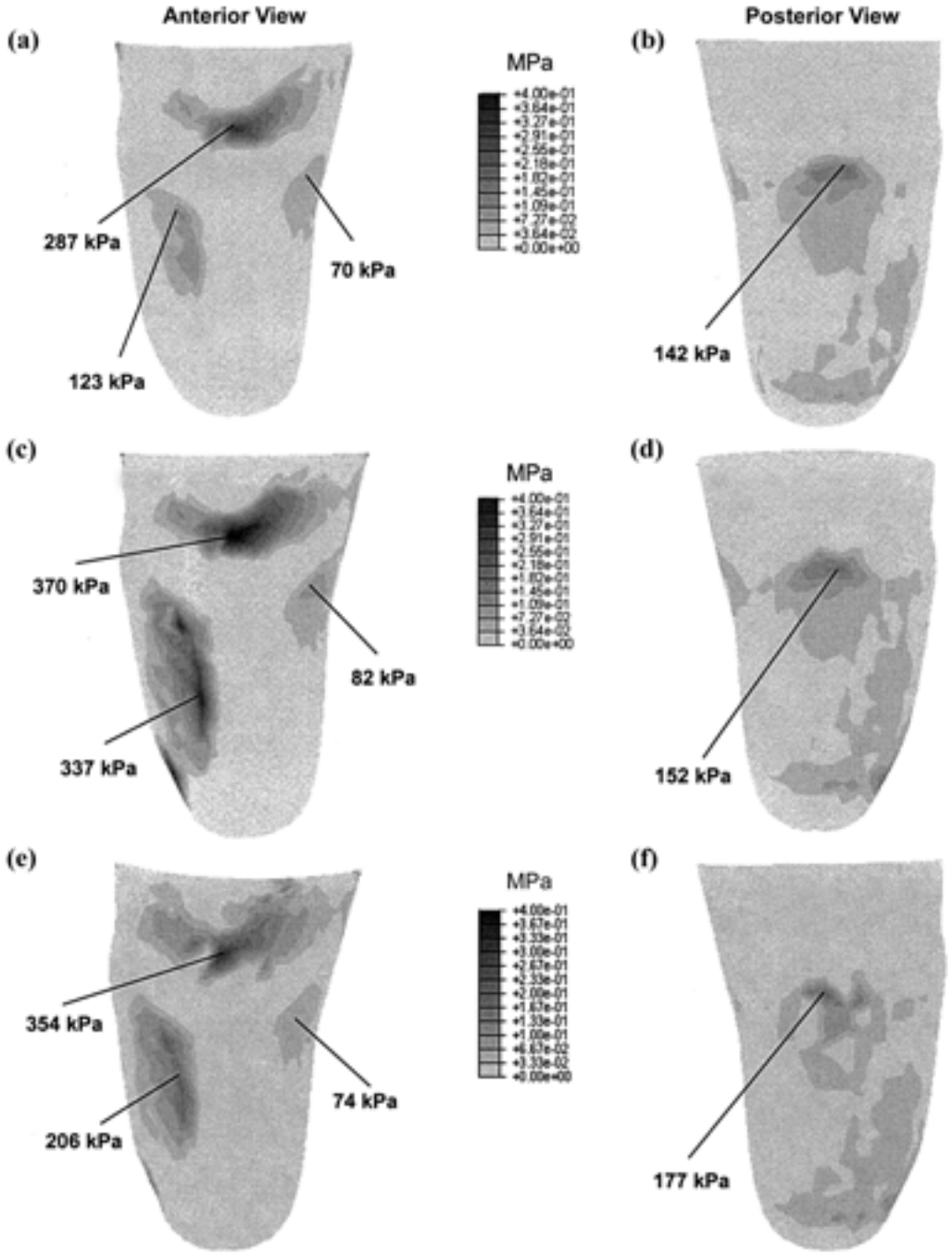

Figure 6.
(a), **(c)**, and **(e)** anterior and **(b)**, **(d)**, and **(f)** posterior views of normal stress distribution at **(a)** and **(b)** heel strike, **(c)** and **(d)** loading response, and **(e)** and **(f)** heel off with monolimb with 48 mm-diameter circular shank.

A monolimb is traditionally fabricated by drape molding of a heated thermoplastic sheet onto the model composed of a shape-modified residual-limb plaster model and a pylon, giving the shape of the socket and the shank of the monolimb [7,9]. A liner can be added within the socket to help distribute stresses more evenly at the limb-socket interface and close the "hole" at the distal end of the socket. However, a liner could cause some problems such as hygiene problems (absorption of sweat) and may require frequent maintenance. We have some

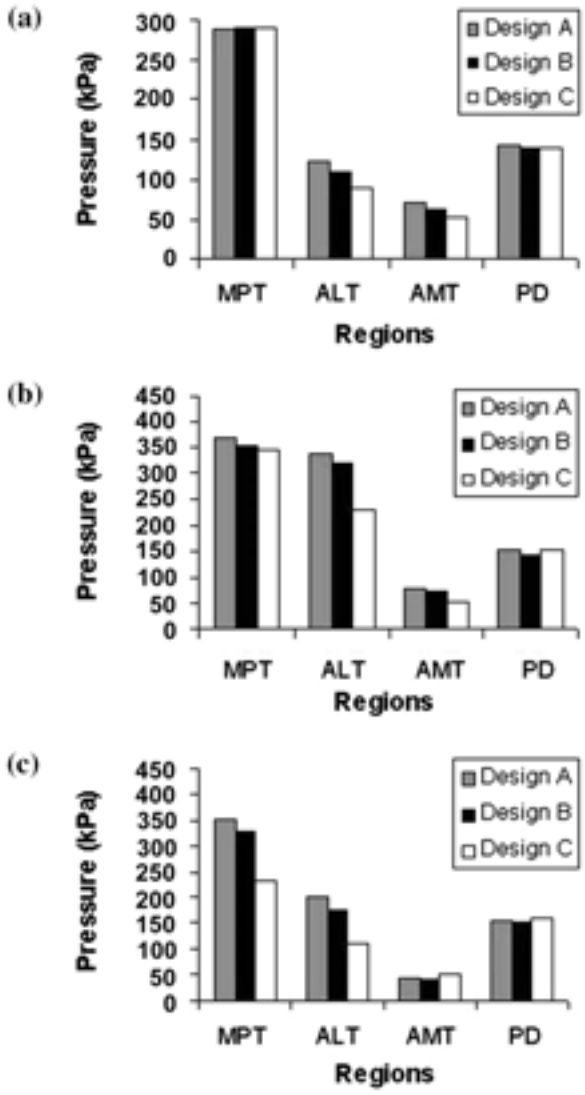

Figure 7.
Comparison of normal stress distribution at mid-patellar tendon (MPT), anterolateral tibia (ALT), anteromedial tibia (AMT), and popliteal depression (PD) regions at **(a)** heel strike, **(b)** loading response, and **(c)** heel off with three different shank designs.

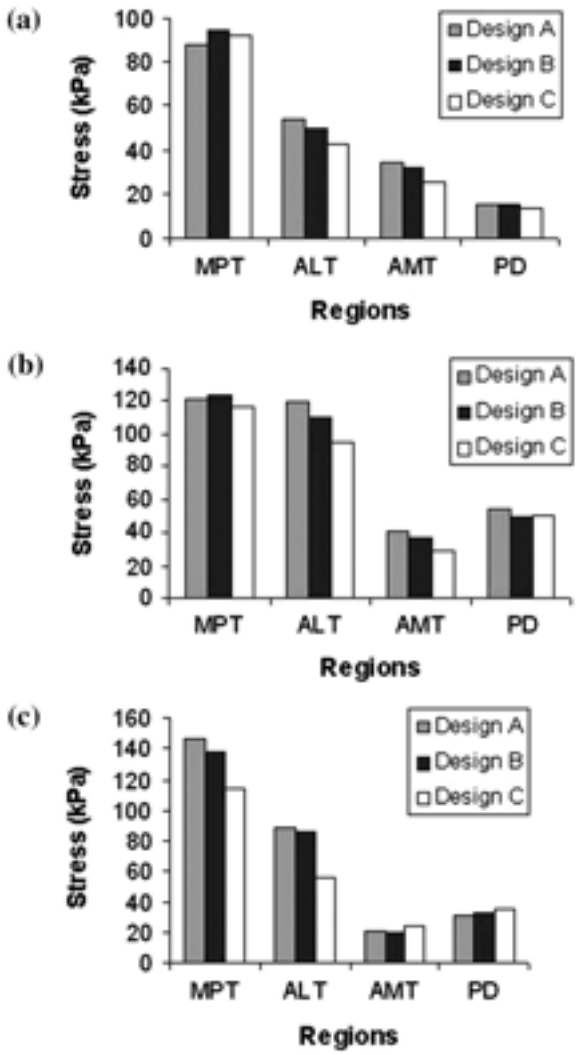

Figure 8.
Comparison of shear stress distribution at mid-patellar tendon (MPT), anterolateral tibia (ALT), anteromedial tibia (AMT), and popliteal depression (PD) regions at **(a)** heel strike, **(b)** loading response, and **(c)** heel off with three different shank designs.

experience in fitting patients with monolimbs that do not have liners, and we do not encounter major fitting problems. For those reasons, a liner was not added in this FE model. Under this fabrication method, the wall-thickness of the thermoplastic material is almost uniform. Adjusting the cross-sectional geometry of the shank of a monolimb appears to be the most effective method of altering the flexibility of the monolimb.

The fabrication processes can be performed with a computer-aided design/computer-aided manufacturing (CAD/CAM) system. The residual limb shape can be digitized, the socket shape modified, and the shank positioned with prosthetic CAD software, such as ShapeMaker™ [30]. The CAD data can then be sent to a rapid prototyping machine for fabrication. The use of rapid prototyping machine to fabricate prosthetic socket has been reported in the literature [31–32]. With CAD/CAM techniques, monolimbs can be tailored to vary wall thickness and geometry of the shank. However, this tailored fabrication method is much more expensive.

In future studies, we will pursue improved characterization of material properties of soft tissues and interface contact conditions between the skin and the socket. Gait analysis and clinical measurement of the stresses at the limb-socket interface and prosthesis will be performed to validate the model. Fatigue life of monolimbs under repeated loading will be investigated. The FE model will be an important tool in optimizing prostheses with flexible shanks. Further parametric analysis of the model will be performed for the optimization.

CONCLUSION

Because of the lack of understanding of the deformation and strength of the shank under loading and the effect the shank deformability on comfort, little has been suggested about the design of a monolimb. In this study, an FE model was developed that can contribute to (1) the prediction of shank deformability of monolimbs during walking without actual prosthetic fitting and direct measurement; (2) the prediction of stress distribution at the shank and the inspection of possible failure of the prosthesis, which serves as a reference for future monolimb design and optimization; and (3) a better understanding of the effect of shank flexibility on socket-limb interaction. An improved understanding of monolimb structural behavior could promote further optimization of the design of monolimbs.

REFERENCES

1. Molen NH. Energy/speed relation of below-knee amputees walking on a motor-driven treadmill. Int Z Angew Physiol. 1973;31:173–85.
2. Waters RL, Perry J, Aatonelli D, Hislop H. Energy cost of walking of amputees: the influence of level of amputation. J Bone Joint Surg. 1976;58A:42–46.
3. Robinson JL, Smidt GL, Arora JS. Accelerographic, temporal, and distance gait: factors in below-knee amputees. Phys Ther. 1977;57:898–904.
4. Bowker JH, Kazim M. Biomechanics of ambulation. In: Moore WS, Malone JM, editors. Lower extremity amputation. Philadelphia (PA): W.B. Saunders Co.; 1989. p. 261–73.
5. Macfarlane PA, Nielsen DH, Shurr DG, Meier K. Perception of walking difficulty by below knee amputees using a conventional foot versus the Flex Foot. J Prosthet Orthot. 1991;3(3):114–19.
6. Menard MR, Murray DD. Subjective and objective analysis of an energy-storing prosthetic foot. J Prosthet Orthot. 1989;1(4):220–30.
7. Valenti TJ. Experience with endoflex: a monolithic thermoplastic prosthesis for below-knee amputees. J Prosthet Orthot. 1991;3(1):43–50.
8. Rothschild VR, Fox JR, Michael JW, Rothschild RJ, Playfair G. Clinical experience with total thermoplastic lower limb prostheses. J Prosthet Orthot. 1991;3(1):51–54.
9. Reed B, Wilson AB, Pritham C. Evaluation of an ultralight below-knee prosthesis. Orthot & Prosthet. 1979;33(2):45–53.
10. Beck JC, Boone DA, Smith DG. Flexibility preference of transtibial amputees. In: Proceedings of the 10th World Congress of the International Society for Prosthetics and Orthotics; 2001 December; Glasgow, Scotland. p. TO9.3.
11. Silver-Thorn MB, Childress DS. Parametric analysis using the finite element method to investigate prosthetic interface stresses for persons with trans-tibial amputation. J Rehabil Res Dev. 1996;33:227–38.
12. Reynolds DP, Lord M. Interface load analysis for computer-aided design of below-knee prosthetic sockets. Med Biol Eng Comput. 1992;30:419–26.
13. Quesada P, Skinner HB. Analysis of a below-knee patellar tendon-bearing prosthesis: a finite element study. J Rehabil Res Dev. 1991;28:1–12.
14. Simpson G, Fisher C, Wright DK. Modeling the interactions between a prosthetic socket, polyurethane liners and the residual limb in transtibial amputees using non-linear finite element analysis. Biomed Sci Instrum. 2001;37:343–47.
15. Zhang M, Lord M, Turner-Smith AR, Roberts VC. Development of a non-linear finite element modeling of the below-knee prosthetic socket interface. Med Eng Phys. 1995;17:559–66.
16. Lee WCC, Zhang M, Jia XH, Boone DA. A computation model for monolimb design. In: Proceedings of the International Society of Biomechanics; 2003; Dunedin, New Zealand. p. 234.
17. Lee WCC, Zhang M, Jia XH, Cheung JTM. FE modeling of the load transfer between trans-tibial residual limb and prosthetic socket. Med Eng Phys. 2004;26:655–62.
18. Jia XH, Zhang M, Lee WCC. Dynamic effects on interface mechanics of residual limb/prosthetic sockets. In: Proceedings of the International Society of Biomechanics; 2003; Dunedin, New Zealand. p. 233.
19. Jia XH, Zhang M, Lee WCC. Load transfer mechanics between trans-tibial prosthetic socket and residual limb—dynamic effects. J Biomech. 2004;37:1371–77.
20. Margolis JM. Engineering thermoplastics: properties and applications. New York: Marcel Dekker Inc.; 1985.
21. Arya AP, Lees A, Nirula HC, Klenerman L. A biomechanical comparison of the SACH, Seattle and Jaipur feet using ground reaction forces. Prosthet Orthot Int. 1995;19:37–45.

22. Lehmann JF, Price R, Bessette SB, Dralle A, Questad K. Comprehensive analysis of dynamic elastic response feet: Seattle Ankle/Lite foot versus SACH foot. Arch Phys Med Rehabil. 1993;74:853–61.
23. Zhang M, Mak AFT. In vivo friction properties of human skin. Prosthet Orthot Int. 1999;23:135–41.
24. Collins JA. Failure of material in mechanical design. New York: John Wiley & Sons; 1993.
25. Perry J. Gait analysis—normal and pathological function. Thorofare (NJ): Slack, Inc.; 1992.
26. Coleman KL, Boone DA, Smith DG, Czerniecki JM. Effect of trans-tibial prosthesis pylon flexibility on ground reaction forces during gait. Prosthet Orthot Int. 2001;25:195–201.
27. Powers CM, Rao S, Perry J. Knee kinetics in trans-tibial amputee gait. Gait Posture. 1998;8:1–7.
28. Zhang M, Turner-Simth AR, Tanner A, Roberts VC. Clinical investigation of the pressure and shear stress on the trans-tibial stump with a prosthesis. Med Eng Phys. 1998; 20:360–73.
29. Convery P, Buis AWP. Conventional patellar-tendon bearing (PTB) socket/stump interface dynamic pressure distributions recorded during the prosthetic stance phase of gait of a trans-tibial amputee. Prosthet Orthot Int. 1998;22:193–98.
30. Boone DA, Harlan JS, Burgess EM. Automated fabrication of mobility aides: review of the AFMA process and DVA/ Seattle Shapemaker software design. J Rehabil Res Dev. 1994;31(1):42–49.
31. Ng P, Lee PSV, Goh JCH. Prosthetic sockets fabrication using rapid prototyping technology. Rapid Prototyping J. 2002;8(1):53–59.
32. Rogers B, Stephens S, Gitter A, Bosker G, Crawford R. Double-wall, transtibial prosthetic socket fabricated using selective laser sintering: a case study. J Prosthet Orthot. 2000;12(3):97–100.

Submitted for publication January 7, 2004. Accepted in revised form May 10, 2004.